Biochimica et Biophysica Acta 1818 (2012) 2192–2201

Contents lists available at SciVerse ScienceDirect

Biochimica et Biophysica Acta

journal homepage: www.elsevier.com/locate/bbamem

Antimicrobial selectivity based on zwitterionic lipids and underlying balance of interactions

Carola I.E. von Deuster, Volker Knecht *

Theory and Bio-Systems, Max Planck Institute of Colloids and Interfaces, Potsdam, Germany

ARTICLE INFO

Article history:
Received 3 November 2011
Received in revised form 26 April 2012
Accepted 9 May 2012
Available online 19 May 2012

Keywords:
Antimicrobial peptide
MD simulation
Selectivity
Membrane
Thermodynamic integration

ABSTRACT

An important feature of antimicrobial peptides is their ability to distinguish pro- from eukaryotic membranes. In vitro experiments on the antimicrobial peptide NK-2 indicate that the discrimination between zwitterionic phosphatidylethanolamine lipids exposed by prokaryotes and phosphatidylcholine lipids exposed by eukaryotes plays an important role. The underlying mechanism is not understood. Here we present molecular dynamics simulations in conjunction with a coarse grained model and thermodynamic integration showing that NK-2 binds more strongly to palmitoyloleoylphosphatidylethanolamine (POPE) than to palmitoyloleoylphosphatidylcholine (POPC) bilayers. Finite size effects on the relative free energy have been corrected for with a method that may also be useful in future studies of the affinities of macromolecules for lipid membranes. Our results support the previous hypothesis that the stronger binding to PE compared to PC arises from a better accessibility of the phosphates of the lipids to the cationic peptide in a sense that a similar number of peptide-lipid salt bridges requires to break more favorable electrostatic headgroup-headgroup interactions for PC relative to PE. The transfer of NK-2 from POPC to POPE is found to lead to a decrease in electrostatic peptide-lipid but an increase in lipid-lipid and ion-lipid interactions, correlating with a dehydration of the lipids and the ions but an increased hydration of the peptide. The increase in affinity of NK-2 for POPE compared to POPC hence arises from a complex interplay of competing interactions. This work opens the perspective to study how the affinity of antimicrobial peptides changes with amino acid sequence and lipid composition.

1. Introduction

With increasing resistances of bacteria against conventional antibiotic treatments, new antibiotical drugs derived from naturally occurring antimicrobial peptides (AMPs) are highly desirable [1]. To use AMPs as drugs is, typically, very expensive and non-amino-acid based peptidomimetic agents that are cheaper to produce are preferable. For a rational design of such antibiotics, it is necessary to understand the function of AMPs in great detail. Many AMPs have been isolated and characterized experimentally and by means of molecular dynamics (MD) simulations [2–6]. AMPs are part of the first line response in the innate immune system of several plants, insects, amphibia and mammals. Common features in AMPs are their relatively small size (between 12 and 60 amino acids), their amphipatic α-helical or β-hairpin structure at membranes, and their large positive charge. AMPs show a broad spectrum of activity against gram positive and negative bacteria, viruses, fungi, and parasites using various different mechanisms to kill the invading pathogens. It has been found that AMPs can interact with extracellular polysaccharides and cell wall components or intracellular targets [6] but the mode of action of most AMPs appears to be the permeabilization of cell membranes through formation of pores above a critical concentration of the peptides on the membrane surface.

An important feature of AMPs is their toxicity against a broad range of microbial targets without affecting the cells produced naturally in multicellular organisms. This antimicrobial selectivity is attributed to a difference in affinity of AMPs for the cytoplasmic membranes of pro- and eukaryotic membranes arising from a difference in lipid composition of the corresponding outer leaflets. A prokaryotic cytoplasmic membrane contains the anionic lipid cardiolipin and phospholipids with either an anionic phosphatidylglycerol (PG) or a zwitterionic phosphatidylethanolamine (PE) headgroup [7]. The outer leaflet of a eukaryotic cell membrane contains sphingomyelin or lipids with the zwitterionic head group phosphatidylcholine (PC) [8]. Antimicrobial selectivity hence partially arises from the presence of anionic lipids in pro- but not eukaryotic membranes, leading to strong attraction of the cationic AMPs to bacterial membranes due to charge complementarity. This view is supported by the finding that bacteria with particularly high concentrations of negatively charged lipids in the outer leaflet are especially susceptible to AMPs [9]. Further support for this view arises from the affinities of AMPs for model membranes

* Corresponding author at: Theory and Bio-Systems, Max Planck Institute of Colloids and Interfaces, Am Mühlenberg 1, 14476 Potsdam, Germany. Tel.: +49 331 5679732; fax: +49 331 5679602.
E-mail address: vknecht@mpikg.mpg.de (V. Knecht).

0005-2736/$ – see front matter © 2012 Elsevier B.V. All rights reserved.
doi:10.1016/j.bbamem.2012.05.012

from *in vitro* experiments [10,11] as well as results MD simulations [12–14].

Nevertheless, marked differences have also been found in the interaction of AMPs with PC or PE lipids although both lipids are zwitterionic. The AMP LL-37 for example perturbs, at intermediate (1-2%) concentrations, palmitoyloleoylphosphatidylethanolamine (POPE) headgroups more strongly than palmitoyloleoylphosphatidylcholine (POPC) headgroups, and it increases the lamellar to inverted hexagonal phase transition temperature in POPE membranes [15]. In contrast, the AMP buforin 2 shows less insertion in POPE membranes than in POPC membranes [2]. Remarkably, a 27-residue AMP derived from the antimicrobial protein NK-lysin shows significant affinity for PE but not for PC bilayers [16,17].

The antimicrobial protein NK-lysin is named after its location of expression which is in natural killer cells of pigs [18]. NK-lysin consists of 78 residues (~9 kDa) and forms five α-helical segments (PDB ID: 1NKL). The highest antimicrobial activity is assigned to the third and fourth α-helix consisting of residues 39 to 65 [19]. A three-fold mutation (L44V, S51T, and W58K) and amidation of this fragment with the amino acid sequence KILRGVCKKIMRTFLRRISKDILTGKK leads to an overall net charge of +10 e and is denoted as NK-2. Experiments display a clear selectivity of NK-2 for gram-positive and gram-negative bacteria but not for human erythrocytes and keratinocytes [19]. MD simulations of NK-2 at dipalmitoyl-PG (DPPG) and dipalmitoyl-PE (DPPE) bilayers show deeper insertion of hydrophobic peptide side chains into the DPPG bilayer [14].

Electrophoresis experiments and biosensor studies by Willumeit *et al.* [16,17] indicate that NK-2 exhibits significant affinity for PG and PE but not for PC. The electrophoresis experiments show that adding NK-2 to PC, PE, or PG vesicles renders the zeta potentials of the vesicles more positive, indicating adsorption of the cationic peptide at the vesicles. The change in the zeta potential compared to the absence of the peptide for DPPC, DPPE, or DPPG vesicles is 6 mV, 25 mV, and 3 mV, respectively, for a peptide:lipid ratio (P:L) in the solution of 1:100, or 9 mV, 50 mV, and 90 mV, correspondingly, for P:L = 1:2 [16]. Hence, in any case, the shift in the zeta potential is larger for PE than for PC, and for the lower value of P:L the shift is even larger for PE than for PG. Also, although NK-2's affinity for pure PG is larger than for pure PE for large P:L values, PE is more abundant in bacterial membranes and, thus, might be of similar importance for NK-2's selectivity as PG.

The mechanism by which NK-2 discriminates between PE and PC, however, is not understood. Willumeit *et al.* hypothesized [16] that the origin for the selectivity could be the smaller size of ethanolamine compared to choline groups, which seems to imply that the anionic phosphate groups of PE are better accessible to the cationic moieties of the peptide than those of PC. This could mean that the number of contacts between the cationic groups of the peptide and the anionic phosphate groups (peptide-lipid salt bridges) is larger whether NK-2 is attached to PE compared to PC. Alternatively, a similar number of peptide-lipid salt bridges could require a stronger perturbation of favorable lipid-lipid interactions if NK-2 is bound to PC compared to PE.

In any case, peptide-lipid salt bridges are only a subset of interactions associated with the binding of NK-2 to phospholipid bilayers; many other interactions contribute as well and their strength might depend on whether NK-2 is attached to PC or PE. Earlier molecular dynamics (MD) studies indicate that molecular association typically arises from a balance of various competing interactions [20–29]. So it would be interesting which interactions favor and which disfavor the binding selectivity of NK-2 for PE compared to PC membranes. Understanding this competition and the mechanism underlying the binding selectivity would not only of fundamental biophysical interest but also be crucial for the rational design of peptide-mimicking antibiotics. To understand the mechanism underlying the selectivity of NK-2 for PE compared to PC we have studied NK-2 bound to PE or PC using MD simulations.

Previous MD simulations on several different proteins revealed insights into protein-membrane binding and addressed the formation of hydrophilic or hydrophobic contacts, the position of proteins within the membrane [30–32], or the free energy of binding between peptides and membranes [33]. Sayyed-Ahmad *et al.* [34] have recently used thermodynamic integration (TI) to study relative binding free energies for the association of different mutant variants of a peptide with micelles, i.e., the shift in binding free energies induced by mutations of the peptide. In their approach, the peptides were simulated in solution and attached to the micelles using an explicit description of the solvent. From the configurations of the peptide and the peptide-micelle complexes corresponding to the end states (free and bound state of the peptide), free energies were calculated using molecular mechanics/Poisson-Boltzmann surface area calculations (end point approach) [35].

An endpoint approach in conjunction with Monte Carlo simulations was employed by Gofman *et al.* to investigate the interaction of NKCS, a derivative of NK-2, with a POPE bilayer [36]. Here, the peptide was treated using a coarse grained description in conjunction with a statistical potential based on available 3D structures of proteins, the membrane was modeled using a continuum description, and an absolute binding free energy was estimated. The specificity of NKCS for POPE compared to POPC, however, was not investigated in that study.

The aim of the present work is to determine the shift in the binding free energy of NK-2 to a lipid membrane induced by a change in lipid composition from POPC to POPE. This requires to simulate the membrane in the presence and absence of the peptide. In contrast to Sayyed-Ahmad *et al.* we do not compute free energies from the end states but from the integration of small free energy changes along an alchemical path (path approach) [37]. The thermodynamic integration using alchemical paths is conducted using a coarse grained (CG) model. A CG model is used in order to be able to access long time scales to sufficiently relax the position of the peptide in the membrane and to minimize the statistical error of the free energy estimate and the estimates for its various components. Our approach is similar to that we have chosen previously to study the relative affinity of NK-2 for PG compared to PC [29]. Our work addresses the following questions: (1) Can the stronger binding of NK-2 to PE compared to PC be reproduced? (2) Does NK-2 bind more strongly to PE than to PC because the cationic moieties of the peptide have better access to the anionic phosphate groups of PE compared to PC? (3) Can the free energy for the binding NK-2 to PE compared to PC be understood from the change of a single component of the free energy or does it result from a competition of opposing interactions? If the latter is the case, which interactions favor stronger binding of NK-2 to PE and which stronger binding to PC?

We find that our simulations reproduce the stronger binding of NK-2 to PE compared to PC, giving confidence in the model employed. However, the cationic moieties of the peptide form less contacts to anionic phosphate groups when attached to PE than when bound to a PC bilayer which would in fact favor the binding of NK-2 to PC. The transfer of NK-2 from POPC to POPE is found to lead to a decrease in electrostatic peptide-lipid interactions but an increase in lipid-lipid and ion-lipid interactions, correlating with a dehydration of the lipids and the ions but an increased hydration of the peptide. Our results show that the free energy for the binding of NK-2 to PE compared to PC cannot be understood from the change of a single component of the free energy but arises from a partial compensation of large opposing terms.

2. Methods

2.1. Setup

The systems studied here are shown in Fig. 1 and included a monocomponent phospholipid bilayer composed of 128 lipids and approximately 2700 CG water beads, corresponding to 10800 water molecules or 84 water molecules per lipid, simulated under periodic boundary conditions. The phospholipid was either POPC or POPE. These systems

were simulated in the absence and in the presence of an NK-2 molecule together with its 10 negative counter ions. The systems simulated are shown in Fig. 1. Excess ions were not included to mimic the low ion concentrations used in the electrophoresis experiments by Willumeit *et al.* [16]. In these experiments, the electrolyte in the solution was 2 mM CsCl. This would correspond to 0.4 two ion pairs in the simulation system which we modeled by not including any excess ions at all. The systems were described using the MARTINI coarse grained model which is based on a four-to-one mapping of heavy atoms to coarse grained beads [38,39]. The lipids and the ions were modeled using MARTINI version 2.0, and the rest was described using MARTINI version 2.1. The model is optimized to match partitioning free energies for small chemical groups; it has been shown to yield good agreement for the partitioning of lipids or individual amino acid side chain analogues in lipid bilayers with atomistic simulations, as well as for the relative partitioning of different dye molecules in lipid bilayers with experimental data [38–40]. We note that the coarse grained approximation for membranes and membrane-protein interactions has recently been documented to be suitable for energy calculations with the thermodynamic integration protocol. Singh and Tieleman [41] have employed the MARTINI model to investigate the partitioning of short peptides at POPC/water interface with thermodynamic integration, free energy perturbation, and umbrella sampling. Within the statistical uncertainty all techniques gave the same results. Thus, in particular thermodynamic integration yielded the same free energies as umbrella sampling which, on the other hand, is well established in the usage in conjunction with the MARTINI model [38–40].

In this model, known or assumed secondary structure elements of peptides are stabilized by appropriate constraints. Circular dichroism spectra and molecular dynamics simulations suggest that NK-2 is α-helical at phospholipid bilayers [14,42]. Hence, the helix-kink-helix structure of the sequence within the parent protein NK-lysin was maintained via dihedral potentials on the backbone stabilizing α-helical conformations except for the residues Thr-13 and Phe-14 representing the kink. A single POPE lipid molecule in coarse grained representation is displayed in Fig. 2, where the *Sn*-1 chain is the saturated tail and consists of four particles. The *Sn*-2 chain is the unsaturated tail with the particle in the third position exhibiting a double bond character.

The simulation protocol was chosen according to standard settings for the MARTINI model. In this model, the polarity of atomic groups is parameterized by effective Lennard-Jones (LJ) potentials of the form

$$V_{\mathrm{LJ}}(r) = 4\epsilon_{ij}\left[\left(\frac{\sigma_{ij}}{r}\right)^{12} - \left(\frac{\sigma_{ij}}{r}\right)^{6}\right] \tag{1}$$

Here, σ_{ij} denotes the closest distance of approach between two particles and ϵ_{ij} the strength of their interaction. The same effective size, $\sigma \equiv 0.47$ nm, is taken for each interaction pair except for the interactions between charged particles and (i) the lipid tails or (ii) leucine, isoleucine, or valine side chains for which $\sigma \equiv 0.62$ nm. The choline particle in POPC and the ethanolamine particle in POPE have the same effective size of 0.62 nm but differ in their interaction strength. The interaction parameter ϵ is larger for ethanolamine than for choline to mimic the hydrogen-bonding capacity of the former. Note that it is not advisable to change the size of the ethanolamine or the choline particle in order to reproduce the size difference between the two atomic groups. This is because the MARTINI model is parameterized carefully to reproduce several bilayer properties and changing one parameter may impair some of these properties. The LJ interactions are truncated at 1.2 nm, and the respective forces decay smoothly to zero between 0.9 and 1.2 nm. The choline and ethanolamine groups of PC and PE lipids as well as the N-terminal backbone bead of NK-2 together with its arginine or lysine side chains exhibit a single positive charge + e. The amidation of the C-terminus of NK-2 was modeled by choosing the C-terminal backbone bead (MARTINI particle type Nd) electrostatically neutral. Cl^- ions together with three water water molecules are modeled as LJ particles with charge -e. Charged coarse grained beads interact via a Coulomb potential that has a relative dielectric constant of 15 and is truncated at 1.2 nm and shifted such that the potential as well as the forces smoothly decay to zero when the cutoff distance is approached.

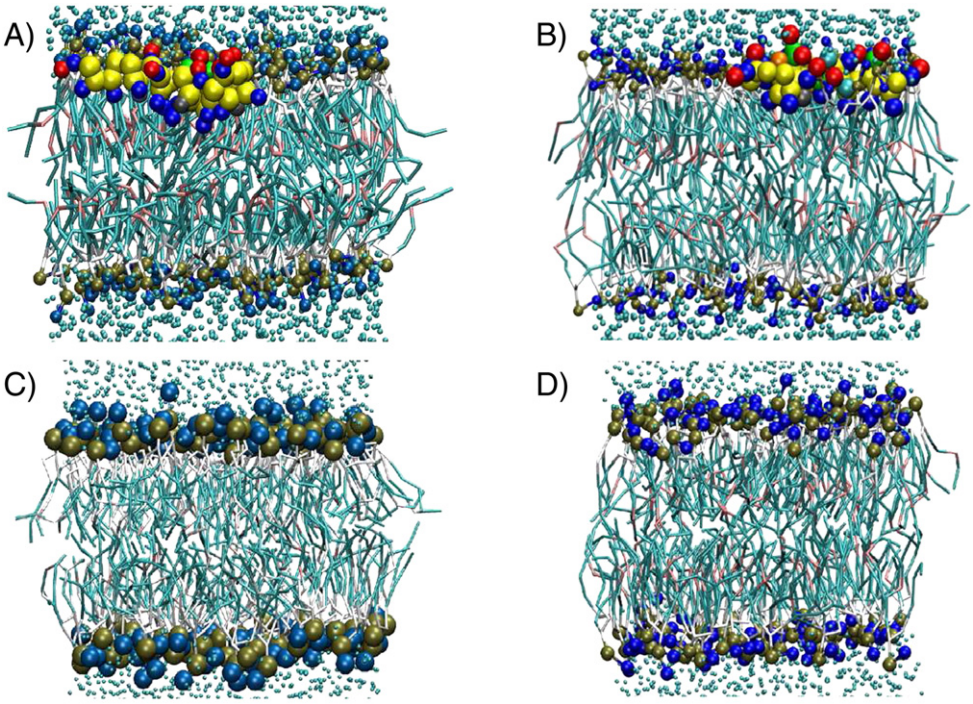

Fig. 1. The simulated systems consisted of a hydrated (A,C) POPC or (B,D) POPE bilayer in (A,B) the presence or (C,D) absence of NK-2. The water is represented as small cyan spheres. The phosphate (brown), the choline (light blue), and the ethanolamine (dark blue) are depicted as spheres, the tails (cyan) and the glycerol backbone (white) of the lipids are shown as sticks. The NK-2 peptide resides at the bilayer water interface and is shown as spheres; colors distinguish between charged (red), nonpolar (blue), and backbone particles (yellow).

To this aim, the Coulomb potential is multiplied by a function that is zero at 1.2 nm such that the interactions decay faster with distance r than $1/r$. In addition to smoothening the interactions this mimics the fact that the inverse dielectric permittivity $1/\epsilon$, though chosen to be distance-independent in the simulations, in reality decreases with distance (reaching the macroscopic value in the asymptotic limit).

The lengths of backbone-side chain bonds of isoleucine, threonine, and valine residues were constrained using the algorithm LINCS [43], which is a linear constraint solver for molecular simulations. This allowed us to use an effective time step of 80 fs for the equilibration and 160 fs for the production runs. We note that all time periods in this paper are given in terms of the effective timescale. The effective timescale is based on the diffusion of lipid molecules and equal to four times the nominal timescale [38]. A grid search algorithm with a 1.2 nm cutoff was used, the corresponding neighbor list being updated every ten steps. A temperature of 310 K was maintained using a Berendsen thermostat [44] with a relaxation time of 0.4 ps (effective timescale). The box size parallel and normal to the bilayer were scaled independently in order to maintain an average pressure of 1 bar in both directions corresponding to a tension-free bilayer using a Berendsen barostat [44] with a relaxation time of 0.8 ps (effective timescale) and a compressibility of 3×10^{-5} bar^{-1}. Positions and velocities of atoms were stored every 5000 steps and the energy every 100 steps. All simulations were carried using GROMACS, version 4.0.7, in double precision [45].

2.2. Thermodynamic Integration

The difference in the affinity of NK-2 for POPE versus POPC was estimated using thermodynamic integration based on the thermodynamic cycle shown in Fig. 3.

If ΔG_{PE} and ΔG_{PC} denote the free energy of adsorption for NK-2 at POPE and POPC, respectively, we computed the difference

$$\Delta\Delta G \equiv \Delta G_{PE} - \Delta G_{PC}. \tag{2}$$

The condition that the free energy change for one cycle is zero,

$$-\Delta G_{PC} + \Delta G_0 + \Delta G_{PE} - \Delta G_p = 0, \tag{3}$$

implies that

$$\Delta\Delta G = \Delta G_p - \Delta G_0. \tag{4}$$

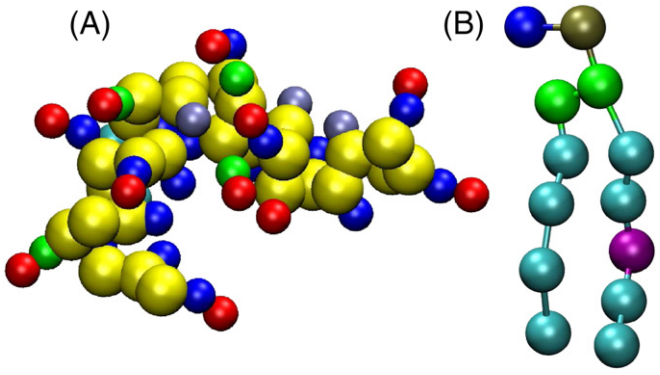

Fig. 2. Coarse grained representation of a NK-2 (A) and a POPE molecule (B). The backbone of the NK-2 peptide is depicted as large yellow spheres. Nonpolar particles in the sidechains are colored in dark blue, cationic side chain particles in red, intermediate polar particles in cyan and light green, and polar particles in gray. The ethanolamine group in POPE is shown in dark blue, the phosphate group in brown, the glycerol backbone in light green, and the hydrocarbon tail particles in cyan for single bond and purple for double bond character.

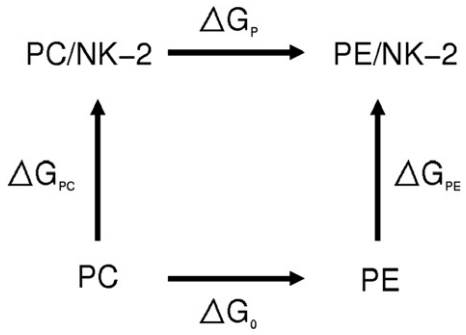

Fig. 3. Thermodynamic cycle based on the four states PC, PC/NK-2, PE, and PE/NK-2 and alchemical transitions between these states. PC/NK-2 and PC refer to the system consisting of a POPC bilayer with and without an attached NK-2 peptide, respectively. PE/NK-2 and PE refer to the analogous systems containing POPE. The quantities ΔG_p and ΔG_0 represent the change in free energy during the transition of POPC to POPE in presence and absence of NK-2. The free energy changes ΔG_{PC} and ΔG_{PE} occur during binding of NK-2 to a POPC and a POPE bilayer, respectively.

This method is corresponds to the general approach used for calculating the difference in binding free energy between a complex AB and a complex AB' by computing the free energy change upon a transformation of B to B′ in the absence and presence of A [37]. In our case, A corresponds to the NK-2 molecule and its ten counterions, while B corresponds to the POPC and B′ to the POPE bilayer.

To get a more intuitive understanding and to facilitate the discussion, we find it useful to look at this procedure from a slightly different perspective. Namely, we want to compute the free energy G_{tr} of the transfer of NK-2 from a POPC to a POPE bilayer, i.e., we study the transition

$$\mathrm{NK2/PC} + \mathrm{PE} \rightarrow \mathrm{PC} + \mathrm{NK2/PE}. \tag{5}$$

Here, PC or PE denote the corresponding peptide-free and NK2/PC or NK2/PE the respective peptide-decorated bilayer. This physical transition can be viewed as a superposition of the alchemical transitions

$$\mathrm{NK2/PC} \rightarrow \mathrm{NK2/PE}. \tag{6}$$

and

$$\mathrm{PE} \rightarrow \mathrm{PC}. \tag{7}$$

According to Fig. 3, the free energy change for the transitions Eqs. (6) and (7) is ΔG_p and $-\Delta G_0$, respectively. The free energy change for the transition Eq. (5) denoted as G_{tr} is the sum of these free energies, hence,

$$G_{tr} = \Delta\Delta G,$$

where $\Delta\Delta G$ is given by Eq. (4). The free energy differences ΔG_P or ΔG_0 in Eq. (4) were computed using thermodynamic integration; a detailed explanation of this method is given in Ref. [46]. In brief, the infinitesimal free energy changes along an alchemical path connecting the corresponding POPC and POPE systems are calculated by defining intermediate POPC-POPE systems using a linear superposition of the respective Hamiltonians. The relative contribution of the corresponding POPC and POPE systems is governed by coupling parameter λ such that $\lambda = 0$ corresponds to the POPC and $\lambda = 1$ corresponds to the POPE system. Simulations for $\lambda = 0, 1$ and at intermediate equidistant λ values with $\Delta\lambda = 0.1$ were conducted. For each λ value, the system was equilibrated for 40 ns and data were collected from the final 1000 ns of a 1600 ns run. The standard error in G_{tr} was determined by dissecting the final 1000 ns of all trajectories into six segments.

2.3. Analysis

The enthalpic contribution H_{tr} to G_{tr} was determined from

$$H_{tr} = U_{tr} + pV_{tr} \tag{8}$$

with pressure p and the volume change V_{tr}. The quantity U_{tr} denotes the corresponding change in the internal energy obtained from

$$U_{tr} = E_{pot,tr} - E_{kin,tr} = E_{pot,tr} \tag{9}$$

where $E_{pot,tr}$ and $E_{kin,tr} = 0$ denote the change in potential and kinetic energy, respectively. The entropic contribution, $-TS_{tr}$, was determined using the Gibbs-Helmholtz equation

$$-TS_{tr} = G_{tr} - H_{tr}. \tag{10}$$

According to Eq. (5), $E_{pot,tr}$ was computed from

$$y_{tr} = \left(y_{PE/NK} + y_{PC}\right) - \left(y_{PE} + y_{PC/NK2}\right), \tag{11}$$

with $y = E_{pot}$. The subscripts PE/NK or PC/NK refer to the systems containing POPE or POPC, respectively, in the presence of NK-2, and PE or PC refer to the corresponding peptide-free systems.

Further analysis was performed in order to elucidate the interactions contributing to $E_{pot,tr}$. For POPC and POPE in the absence and presence of the peptide, we computed the number of contacts N between the groups considering pairs of beads with separations below 0.5 nm, as well as the electrostatic and the LJ energies E_{el} and E_{LJ}, respectively, from the interactions between these groups. The corresponding changes in these variables upon the transfer Eq. (5) were calculated according to Eq. (11) with $y = N$, E_{el}, or E_{LJ}.

The standard error of $y_{PE/NK}$, y_{PC}, y_{PE}, and $y_{PC/NK2}$ in Eq. (11) was computed from block averages, dissecting the trajectories into four segments. The standard error of y_{tr} and $-TS_{tr}$ was determined via error propagation.

The number densities for various groups normal to the bilayer were determined by choosing a bin width of 0.06 nm and normalizing each density profile such as to be one at the maximum.

3. Results and discussion

3.1. Orientation of NK-2

To obtain the initial configuration for the thermodynamic integration simulations, NK-2 was placed in bulk water close to a POPE bilayer with the cationic lysine and arginine residues facing the membrane surface. During the simulation, the peptide changed its orientation and attached first with the hydrophobic side chains of residues 14 to 27 at the POPE bilayer. The helix consisting of residues 1 to 13 initially extends into the water and forms an angle of 40° with the membrane surface. During the simulations the helix moves towards the membrane and eventually attaches to it. The cationic residues lysine and arginine as well as the amidated C-terminus faced the water solution. The partitioning of the peptide in the headgroup region and its parallel alignment with the membrane is in agreement with data for NK-2 at phospholipid monolayers from X-ray scattering experiments [42] and previous molecular dynamics simulations [14,36]. The latter references, in particular, also indicated that NK-2 at phospholipid bilayers prefers to insert its nonpolar side chains into the membrane while exposing its charged side chains to the water.

The time evolution of the penetration of NK-2 into POPC and POPE in terms of the corresponding center of mass distances normal to the bilayer is depicted in Fig. 4B. In the initial configuration of these simulations, NK-2 already adopts the correct orientation, i.e., its hydrophobic face points toward the membrane. NK-2's first helix formed by residues 1 to 13 inserts into the POPE bilayer after 120 ns and into the POPC bilayer after 600 ns. It seems that NK-2 attaches more slowly but more deeply into the POPC bilayer than into the POPE bilayer. Fig. 4A shows the distribution of selected groups of the lipids and the peptide normal to the bilayer for the leaflet, at which NK-2 is attached, averaged over the final 1000 ns. The distributions indicate stable phospholipid bilayers for all systems. In particular, no water or lipid headgroup is observed in the hydrophobic interior of the bilayer; which implies the absence of pore formation. The choline, ethanolamine, and phosphate groups reside at the interface between the water and the lipid tails. The distributions of the choline or ethanolamine and the phosphate groups overlap, the cationic groups showing a tail toward the water phase. The tail is somewhat more extended for cholines than for ethanolamines, indicating the stronger hydration of the former. For decreasing distances from the center of the bilayer, the water density decays from the value in the bulk to essentially zero with a shoulder at the location of the phosphate groups, the shoulder being higher for POPC than for POPE.

For POPC, the distribution of the lysine or arginine residues as well as the N-terminus of the peptide coincide with the distribution of the choline groups of the lipids. In contrast, the nonpolar residues reside at the interface between the head groups and the tails of the lipids. NK-2 at POPE shows a similar behavior, except for the distribution of the cationic residues which is overall broader than for POPC. Overall, these results highlight the amphipathic nature of NK-2 and the favorable partitioning of its polar and nonpolar side at the interface. Counter ions of the peptide distribute freely in solution but do show an affinity for the peptide. For POPE the ions accumulate more strongly in the vicinity of the peptide than for POPC. The average angle between the two helices of the helix-kink-helix structure of NK-2 and the corresponding standard deviations are $110° \pm 6°$ at POPC and $121° \pm 4°$ at POPE.

3.2. Effect of peptide on POPC and POPE bilayers

Table 1 shows the area per lipid for POPE or POPC in the absence and presence of the peptide.

The area per lipid was 0.653 nm^2 for POPC and 0.617 nm^2 for POPE in our CG simulations. Previous atomistic simulations yielded 0.665 nm^2 for POPC and 0.545 nm^2 for POPE [47]. Experimental values at 30 °C are 0.683 nm^2 for POPC [48] and 0.56 nm^2 for POPE [49]. It should be noted that experimental values of areas per lipid can be determined by different methods and the resulting estimates differ by up to 13% in the case of PC lipids [50,47–49]. Though giving a smaller absolute value for the difference in areas per lipid between POPC and POPE, the simulations do reproduce the lower area for POPE as indicated experimentally.

Upon adsorption of NK-2, the area per lipid increases by 1 – 2 %. The increase in area per lipid likely arises from the addition of material in the leaflet to which the peptide is bound. Changes in the area per lipid correlate with the order of lipid tails as described in the Supplementary Material. The area per lipid also correlates with the depth to which NK-2 penetrates into the bilayer as shown in Fig. 4A. The larger area of POPC correlates with a deeper insertion of NK-2 into the bilayer.

3.3. Thermodynamics of binding selectivity

Although the PC and PE head groups have a very similar atomic structure, previous experiments indicate significant differences in the corresponding binding affinities for NK-2. Here we will compare the relative free energy for the binding of NK-2 to PE compared to PC from our simulations to a value for a related system derived from experimental data.

3.3.1. Binding selectivity from simulation

The relative binding free energy for the binding of NK-2 to POPE compared to POPC is the difference between the corresponding binding

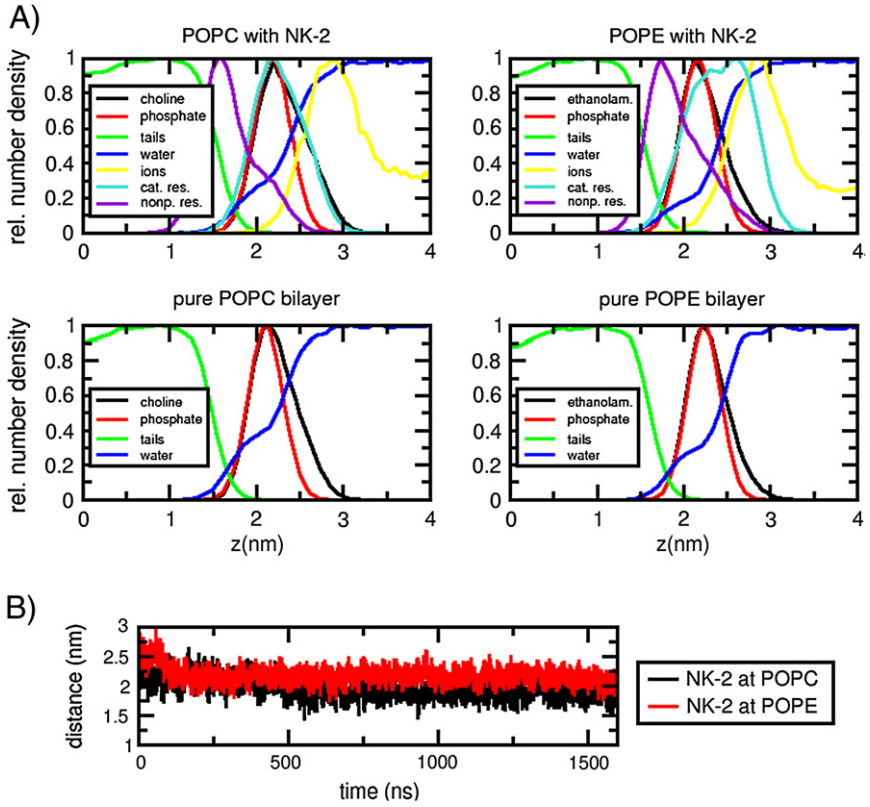

Fig. 4. A) Number densities of POPC and POPE bilayers as a function of the distance z from the center of the bilayer, scaled to the maximum. The contributions from selected groups of NK-2 are shown only for positive values of z. B) In addition, the center of mass distances of the peptide to the POPC and POPE bilayers are plotted as a function over time. For data analysis the time frames from 600 ns to 1600 ns are used.

energies, or, which is equivalent, equal to the free energy change for the transfer of NK-2 from a POPC to a POPE bilayer, as explained in the Methods. We have computed this free energy change using thermodynamic integration. Fig. 5 shows the difference in the derivative of the free energy with respect to the coupling parameter λ between the system with and without the peptide, as a function of λ. The curve is smooth, suggesting that simulations at eleven equally spaced λ values are sufficient to resolve the free energy profile $G(\lambda)$. Integration of the curve using the trapezoidal method yields a free energy of transfer of $G_{tr} = -10 \pm 1$ kJ/mol, see Table 2. The negative value of G_{tr} indicates a stronger binding of NK-2 to POPE than to POPC bilayers. Hence, our model reproduces the experimental finding that NK-2 binds more strongly to PE than to PC model membranes [16,17].

3.3.2. Free energy decomposition

Further decomposition of the free energy may reveal the interactions that support or oppose the binding selectivity. The enthalpic contribution to G_{tr} as calculated from Eq. (9) is $U_{tr} = -26 \pm 13$ kJ/mol and the entropic component from Eq. (10) is $-TS_{tr} = 16 \pm 13$ kJ/mol. Hence, the change in free energy arises from a partial compensation of large energetic and entropic terms, and the statistical error of the energetic and entropic components is one order of magnitude larger than that of the free energy itself; both effects are common in free energy calculations by MD simulations [20–26,51,52]. The sign of G_{tr} is determined by the energetic contribution. The results are summarized in Table 2.

It must be noted that the decomposition of the free energy into enthalpy and entropy has to be interpreted with care. The entropic contribution determined from the coarse grained simulations is not expected to be the same as would be measured experimentally, due to the fact that some contributions which are entropic in experiment (presumably mainly arising from water orientation related to hydrophobic and electrostatic effects [53]) are contained in the enthalpic component for the coarse grained model due to the averaging over some degrees of freedom. The question whether certain components are entropic or enthalpic is anyway secondary in the given context. The decomposition of the free energy into an entropic and an enthalpic component is just the first step for an even

Table 1
Average area per lipid (in nm^2) of the POPC and POPE bilayer, in the presence and absence of NK-2. *CG* refers to the coarse grained simulations, *A* to previous atomistic simulations [47].

	POPC	POPE
With NK-2 (CG)	0.669±0.01	0.626±0.008
Without NK-2 (CG)	0.653±0.01	0.617±0.008
Without NK-2 (A)	0.665 nm^2	0.545 nm^2

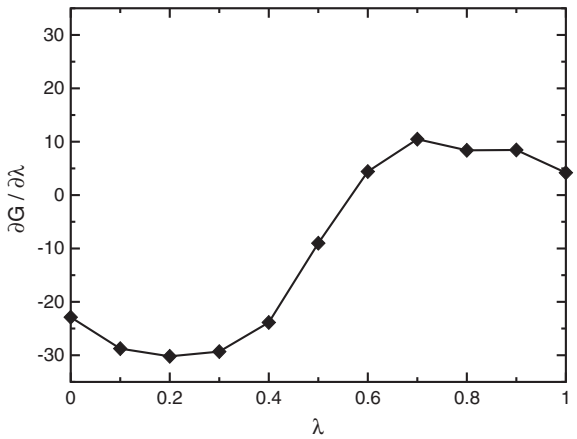

Fig. 5. Difference in the derivative of the free energy with respect to the coupling parameter λ between the system containing the peptide and the peptide-free system, $\partial G/\partial\lambda = \partial G_p/\partial\lambda - \partial G_0/\partial\lambda$, as a function of λ.

Table 2
Change in free energy upon transfer of NK-2 from a POPC to a POPE bilayer, G_{tr}, as well as corresponding mechanical, energetic, and entropic contributions, pV_{tr}, U_{tr}, and $-TS_{tr}$, respectively, from thermodynamic integration, in kJ/mol.

G_{tr}	-10 ± 1
$-TS_{tr}$	16 ± 13
U_{tr}	-26 ± 13
pV_{tr}	-1 ± 7

more detailed decomposition into various contributions which allowed us to identify the interactions favoring and opposing the binding selectivity. The mechanical contribution to the enthalpic component is $pV_{tr} = -1 \pm 7$ kJ/mol. Entropic contributions within the coarse grained model used here are discussed in the following and energetic contributions in the subsequent section.

3.4. Entropy decomposition

In order to partially decompose the entropic contribution, we subdivide our system into peptide, ions, and the rest, being the water and the lipids. The entropy is the sum of contributions from correlations within and between these subcomponents. The contribution from peptide-peptide correlations, the "peptide entropy", shall be denoted as $S_{P,tr}$. The contribution from ion-ion correlations, the "ion" entropy, will be called $S_{I,tr}$. The remaining entropic contribution, the "rest" entropy, shall be denoted as $S_{S,tr}$. By definition, the total entropy is the sum of these components,

$$S_{tr} = S_{P,tr} + S_{I,tr} + S_{S,tr} \tag{12}$$

One degree of freedom of the peptide is the kink between the two helical segments which will contribute to the peptide entropy. The average kink angle as well as the corresponding standard deviations are $110^\circ \pm 6^\circ$ at POPC and $121^\circ \pm 4^\circ$ at POPE. The corresponding entropy change is calculated from the corresponding covariance matrix for the peptide coordinates. The covariance matrix contains the correlations between the original Cartesian coordinates as off-diagonal elements. However, the covariance matrix is diagonalized. The eigenvectors of the matrix correspond to collective motions which, by construction, are uncorrelated. Hence, the peptide entropy is the sum of the entropies of these collective motions, approximated to be harmonic. We obtain $-TS_{P,tr} = -7.8 \pm 2$ kJ/mol.

The entropy change of the ions was determined from the spatial distribution of the ions normal to the bilayer, $\rho(z_i)$, where the ion density profiles have been normalized such that

$$\sum_i p_i = 1 \quad \text{and} \quad p_i = \text{const} \times \rho(z_i) \tag{13}$$

where i is the index of the bin. The difference in ion distribution is calculated according to

$$S_{I,tr} = N\left(S_{I,PE} - S_{I,PC}\right) \tag{14}$$

with the entropies

$$S_{I,k} \equiv -R \sum_i p_i \ln p_i, \quad k = \text{PC, PE}. \tag{15}$$

Here, R denotes the universal gas constant and $N = 10$ the number of ions in the system. The assumption used here is that each ion moves in the effective field of the rest of the system and that correlations between the ions are insignificant. The latter assumption seems to be justified for the low ion concentration used here. The motivation to determine the entropic component of the ions from the ion density profile $\rho(z)$ was that this profile is more localized for POPE than for POPC as shown in Fig. 4 of the manuscript (indicating a stronger adsorption of ions at the POPE bilayer), which implies a decrease in translational entropy in the z direction. Using the relation (14), the corresponding entropy change is found to be $-TS_{I,tr} = +6.2 \pm 3$ kJ/mol. The rest entropy from Eq. (12) is $-TS_{S,tr} = +18.5 \pm 13$ kJ/mol.

3.5. Energetic interactions favoring and opposing preferential binding of NK-2 to POPE compared to POPC

In order to identify factors favoring and opposing the stronger binding of NK-2 to POPE compared to POPC, we divided the systems into various subsystems; here we distinguished the phosphate and the choline/ethanolamine groups as well as the tails of the lipids, the water, the cationic and nonpolar moieties of the peptide, and the anions. For POPC and POPE in the absence and presence of the peptide, we computed the number of contacts N between the groups considering pairs of beads with separations below 0.5 nm, as well as the electrostatic and the LJ energies E_{el} and E_{LJ}, respectively, from the interactions between these groups. The process of interest is the transfer of NK-2 from POPC to POPE as described in Eq. (5). The changes in the observables upon the transfer of NK-2 from POPC to POPE denoted as transfer values N_{tr}, $E_{el,tr}$, and $E_{LJ,tr}$, were computed according to Eq. (11).

It should be noted that in the coarse grained model used here, the LJ interactions also encode the polarity of the corresponding chemical groups.

The values for contact numbers for peptide-free POPC and POPE bilayers, as well as the difference between the POPC and the POPE system, are shown in Table S1. The contact numbers for POPC and POPE in the presence of the peptide, as well as the difference between the POPC and the POPE system, are given in Table S2. The results for N_{tr} are shown in Table S3. The values for the electrostatic interactions for the individual systems and their change upon the transfer are given in Table S4. The results for the LJ interactions for the individual systems and their change upon the transfer are given in Table S5.

In general, the magnitudes of the numbers are often large for the individual systems while largely canceling for the differences $\Delta y_{NK} \equiv y_{PE/NK} - y_{PC/NK}$ and $\Delta y_0 \equiv y_{PE} - y_{PC}$, and the Δy_{NK} and Δy_0 largely cancel in the difference $y_{tr} = \Delta y_{NK} - \Delta y_0$. Nevertheless, the individual energetic values $E_{el,tr}$ and $E_{LJ,tr}$ are often of the same order of magnitude or even larger in size as the net transfer energy U_{tr}, either supporting (< 0) or opposing (> 0) the binding selectivity.

As found here, it is commonly observed in MD simulations that individual components of the energy are larger in size than the total energy [20–23,25,26] and associated with larger statistical errors [23,25]. In particular, Horinek *et al.* found that for the binding of a mildly hydrophobic peptide to a flat hydrophobic surface, individual energy contributions almost completely canceled [23]. As in that case, the stronger binding of NK-2 to POPE compared to POPC studied here appears to arise from a subtle balance of interactions. That the statistical error of the free energy is typically significantly smaller than that of its individual components indicates that the fluctuations of the components are correlated and therefore largely cancel out in the statistical error of the free energy.

3.5.1. Transfer of NK-2 from POPC to POPE leads to decrease in peptide-lipid interactions

Unexpectedly, the transfer is found to weaken important peptide-lipid interactions. After the transfer, the cationic moieties of the peptide form less contacts with the phosphate groups of the lipids ($N_{tr} = -0.7 \pm 0.1$, $E_{LJ,tr} = +14 \pm 1$ kJ/mol), yielding an unfavorable electrostatic contribution of $E_{el,tr} = +15 \pm 1$ kJ/mol. The transfer is also found to decrease the number of contacts between the nonpolar moieties of the peptide and the lipids ($N_{tr} = -1.3 \pm 0.1$, $E_{LJ,tr} = 24 \pm 3$ kJ/mol). The latter correlates well with the deeper insertion of NK-2 into POPC compared to POPE shown in Fig. 4. However, not only the peptide-lipid, but also all other

interactions contribute to the transfer free energy and enthalpy which are found to be favorable overall. The most important other contributions are discussed in the following.

3.5.2. Transfer leads to increase in electrostatic lipid-lipid interactions

After the transfer, the (anionic) phosphate groups of the lipids form more contacts with the (cationic) choline/ethanolamine groups of the lipids ($N_{tr} = +1.8 \pm 0.2$ and $E_{LJ,tr} = -23 \pm 3$ kJ/mol). The corresponding electrostatic contribution is $E_{el,tr} = -37.5 \pm 3.7$ kJ/mol.

3.5.3. Transfer leads to increase in ion-lipid interactions

As discussed above, the density profiles shown in Fig. 4 indicated that the counteranions of the peptide more strongly accumulate at the bilayer when NK-2 is attached to POPE. This is reflected in increased (unfavorable) electrostatic interactions of the ions with the phosphate groups ($E_{el,tr} = 4.6 \pm 0.7$ kJ/mol) and increased (favorable) electrostatic interactions of the ions with the choline/ethanolamine groups ($E_{el,tr} = -5.9 \pm 1.6$ kJ/mol).

3.5.4. Transfer leads to dehydration of lipids and ions but increased hydration of peptide

The decreased peptide-lipid interactions correlate with increased peptide-water interactions. After the transfer, the water forms more contacts with the cationic and the nonpolar moieties of the peptide ($N_{tr} = 0.6 \pm 0.1$ and $E_{LJ,tr} = -32 \pm 2$ kJ/mol for the cationic as well as $N_{tr} = 1 \pm 0.1$ and $E_{LJ,tr} = -12 \pm 2$ kJ/mol for the nonpolar groups of NK-2). On the other hand, the increased lipid-lipid and ion-lipid interactions correlate with decreased lipid-water and ion-water interactions. After the transfer the water forms less contacts with choline/ethanolamine groups ($N_{tr} = -1.9 \pm 0.4$, $E_{LJ,tr} = +75 \pm 7$ kJ/mol), phosphate groups ($N_{tr} = -1.1 \pm 0.4$, $E_{LJ,tr} = 57 \pm 10$ kJ/mol), and lipid tails ($N_{tr} = -1.7 \pm 0.5$, $E_{LJ,tr} = 17 \pm 3$ kJ/mol). A contribution of $E_{LJ,tr} = 16 \pm 2$ kJ/mol arises from the ion-water interactions. The decreased water-lipid and water-ion interactions correlate with a strong increase in water-water interactions ($N_{tr} = 13 \pm 6$, $E_{LJ,tr} = -76 \pm 17$ kJ/mol).

Besides the values discussed here, also smaller transfer energy values from other interactions supporting or opposing the binding selectivity were dissected as given in table S4 and S5.

3.6. Discussion of previous hypothesis for selectivity mechanism

Willumeit *et al.* [16,17] attribute NK-2's increased affinity to PE lipids to the smaller size of the amine group in ethanolamine compared to the voluminous trimethylamine moiety in choline, rendering the phosphates of the lipid head groups better accessible for the cationic moieties of the peptide. Our simulations show that this is true in the sense that the number of favorable contacts between anionic phosphate groups and the cationic moieties of the lipids is smaller if NK-2 is attached to PC compared to PE. On the other hand, the number of peptide-lipid salt bridges is not smaller but even larger if NK-2 is bound to PC compared to PE. Overall, the selectivity of NK-2 is determined by a subtle interplay of competing interactions.

3.7. Quantitative comparison with experiment

3.7.1. Binding selectivity for large lipid per peptide ratios

The binding of the peptide to one leaflet (*cis* leaflet) will lead to a tendency of this leaflet to expand, whereas the equilibrium area for the other leaflet (*trans* leaflet) will remain unchanged. Under the (periodic) boundary conditions chosen here, the total area of the *cis* and the *trans* leaflet adopted after binding of the peptide will be the same and be a compromise between the deviations from the equilibrium areas of the *cis* and the *trans* leaflet. The resulting frustration may be released by exchange of lipids between the leaflets which, however, is very slow (taking place on a timescale of hours). This frustration effect will, on the other hand, reduce the affinity of the peptide for the membrane. The effect will be present both for PC and PE but possibly with a different magnitude, shifting the transfer free energy G_{tr} by some amount $G_{tr,f}$. In principle, this effect will occur not only in the simulations but also, though with smaller magnitude, in the experiments, as we will show below.

The value of the transfer free energy after correcting for the area frustration effect shall be denoted as the *intrinsic* binding free energy, $G_{tr,i}$, which thus is given by

$$G_{tr,i} = G_{tr} - G_{tr,f}. \tag{16}$$

As shown in section S2, the area frustration-induced shift in the transfer free energy depends on the number of lipids per leaflet and peptide (lipid per peptide ratio), N. In the simulations, $N = 64$ is the same for PE and PC, yielding

$$G_{tr,f,MD} = \frac{g_{PE} - g_{PC}}{N}, \tag{17}$$

where

$$g_i = \frac{K_{A,i} b_i^2}{8a}, i = \mathrm{PC}, \mathrm{PE}. \tag{18}$$

Here, $K_{A,PC}$ or $K_{A,PE}$ denotes the area compressibility modulus of a POPC or POPE bilayer, respectively. The symbol b_{PC} or b_{PE} shall denote the effective area of the peptide which is the area increase of a POPC or POPE bilayer, correspondingly, if one NK-2 molecule would bind to each leaflet of the bilayer. The effective area of the peptide is obtained from

$$b_i = 2\left(A_i - A_{i,0}\right), i = \mathrm{PC}, \mathrm{PE}, \tag{19}$$

where A_{PC} or A_{PE} is the total projected area of the POPC or the POPE bilayer with NK-2 bound at one side, and $A_{0,PC}$ or $A_{0,PE}$ is the projected area of the peptide-free POPC or POPE bilayer, correspondingly. The area compressibility modulus of a bilayer can be calculated from the standard deviation of the area per lipid of a peptide-free bilayer, σ_A, and the corresponding average area, $A_{0,i}$, via [54]

$$K_{A,i} = \frac{A_{0,i} k_B T}{\sigma_{A,i}^2}, i = \mathrm{PC}, \mathrm{PE}. \tag{20}$$

In the experiments, the different affinities of NK-2 for PE and PC lead to different corresponding numbers of lipids per leaflet per peptide, N_{PC} and N_{PE}. This yields

$$G_{tr,f} = \frac{g_{PE}}{N_{PE}} - \frac{g_{PC}}{N_{PC}}. \tag{21}$$

As shown in Table 3, the area compressibility moduli for POPC (540 ± 30 dyn/cm) and that for POPE (590 ± 90 dyn/cm) are the same within the error, whereas the effective area of the peptide is larger for POPC (2.06 nm^2) than for POPE (1.17 nm^2). This yields $g_{PC} = 2.64(\pm 0.16) \times 10^2$ kJ/mol and $g_{PE} = 0.98(\pm 0.15) \times 10^2$ kJ/mol and, hence, $G_{tr,f} = -2.60(\pm 0.35)$ kJ/mol. The transfer free energy in the limit of large lipid to peptide ratios is thus $G_{tr,i} = -7.40(\pm 1.06)$ kJ/mol.

Table 3
Effective area of NK-2 when attached to POPC or POPE bilayer, b, and area compressibility moduli for POPC or POPE bilayer from our simulations, K_A.

	POPC	POPE
b (nm^2)	2.0637 ± 0.0076	1.1676 ± 0.0067
K_A (dyn/cm)	539 ± 33	589 ± 91
g (10^2 kJ/mol)	2.6	1.0

3.7.2. Binding selectivity from experiment

As experimental data on the binding affinities of NK-2 for POPC or POPE are not available, we will compare our results to data for the interaction of NK-2 with other PC and PE lipids, DPPC and DPPE, from electrophoresis experiments [16]. These experiments showed a change in the zeta potential of lipid vesicles relative to the peptide-free case for a peptide:lipid ratio of 1:100 of 6 mV for DPPC and 25 mV for DPPE. From the zeta potential ζ of a vesicle, the surface charge σ of the vesicle may be estimated from the Grahame equation [55],

$$\sigma = \frac{\epsilon_0 \epsilon \zeta}{\lambda_D}. \tag{22}$$

Here, ϵ_0 is the static dielectric permittivity of the vacuum and ϵ the relative permittivity of water which is 80.1 at 20 °C. The symbol λ_D denotes the Debye length which for a 1:1 electrolyte reads

$$\lambda_D = \sqrt{\frac{\epsilon\epsilon_0 k_B T}{e^2 2c}}. \tag{23}$$

Here, k_B denotes the Boltzmann constant, T the temperature, e the elementary charge, and c the electrolyte concentration which was $c = 2$ mM in the experiments. The binding free energy ΔG for the association of NK-2 with the vesicles is related to the ratio of the concentration of bound peptides at the surface $c_{pep,b}$ and the concentration of peptides in the bulk c_{pep} according to

$$\Delta G = -k_B T \ln \frac{c_{pep,b}}{c_{pep}}. \tag{24}$$

Here, $c_{pep,b}$ may be expressed in terms of the area density of bound peptides at the surface, Γ, and the translational freedom of bound peptides normal to the membrane-water interface, Δz, as $c_{pep,b} = \Gamma/\Delta z$ [56]. The area density of bound peptides at the surface is related to the surface charge of the vesicle as $\Gamma = \sigma/q$ where $q = 10e$ denotes the charge of a single peptide. Denoting the free energy of binding NK-2 to DPPE or DPPC by ΔG_{PE} or ΔG_{PC}, respectively, and the area density of bound peptides at the surface of DPPE or DPPC vesicles by Γ_{PE} or Γ_{PC}, correspondingly, and using Eq. (24), leads to the expression

$$G_{tr,exp} \equiv \Delta\Delta G \equiv \Delta G_{PE} - \Delta G_{PC} = -k_B T \ln \frac{\Gamma_{PE}}{\Gamma_{PC}}. \tag{25}$$

From the measured changes in zeta potentials and the equations above the value $G_{tr,exp} = -3.6$ kJ/mol is obtained. From the area density of bound peptides at the surface, Γ, and the experimental value for areas per lipid for POPC or POPE, a, the corresponding number of lipids per leaflet and bound peptide, N, is estimated according to $N = 1/a\Gamma$. This yields $N = 3800$ for POPC and $N = 1100$ for POPE. For better comparison with the experimental transfer energy we may extrapolate the area frustration energy for the systems studied to these experimental numbers of lipids per leaflet and bound bound peptide. With Eq. (21) we obtain $G_{tr,f,exp} = 0.019(\pm 0.013)$ kJ/mol. This indicates that for the experimental lipid per peptide ratios the area frustration energy for our systems are small compared to the statistical error of our transfer free energy estimate and therefore negligible.

Hence it is appropriate to compare the experimental value for the transfer free energy to the finite size corrected value of the transfer free energy from our simulations. We note that we have compared POPE with POPC which were in the biologically relevant fluid phase whereas the experiments [16] considered DPPE and DPPC at conditions where these lipids were in the biologically less relevant gel phase, so quantitative agreement may not be expected. We find that the free energy for the transfer of NK-2 from POPC to POPE from our simulations is two-fold larger in size compared to the experimental value for the transfer from DPPC to DPPE. This may indicate that under biologically relevant conditions NK-2's selectivity for PC compared to PE is even more pronounced than suggested by the experiments.

4. Conclusion

This study demonstrates the utility of coarse grained MD simulations in conjunction with the thermodynamic integration method to study the difference in binding affinities of the NK-2 peptide to POPC and POPE bilayers. It extends the studies of Pimpthon *et al.* [14] where the binding of NK-2 to DPPG and DPPE bilayers is monitored using nonbonded interaction energies. Our molecular dynamics simulations reproduce the higher affinity of NK-2 for POPE compared to POPC, giving confidence in the model employed. The corresponding difference in binding free energies is $G_{tr} = -10 \pm 1$ kJ/mol for the membrane patch considered here, and correcting for finite size effects yields an intrinsic difference in binding free energies of $G_{tr,i} = -7.40(\pm 1.06)$ kJ/mol. The method used to correct for finite size effects here may also be employed in future studies of the affinities of macromolecules for lipid membranes.

Willumeit *et al.* attributed the higher affinity of NK-2 for PE to a better accessibility of the phosphate groups to the cationic side chains of the peptide. We find that this is true in a sense that a similar number of phosphate-peptide salt bridges requires a stronger perturbation of favorable lipid-lipid (phosphate-cationic group) interactions when NK-2 is attached to PC compared to PE. It might be generally expected that the increase in affinity of NK-2 for POPE compared to POPC arises from a complex interplay of competing interactions. Based on a detailed analysis we have identified the interactions supporting and opposing NK-2's selectivity for PE compared to PC. Though the transfer of NK-2 from PC to PE is found to lead to a decrease in electrostatic peptide-lipid interactions it yields an increase in lipid-lipid and ion-lipid interactions, correlating with a dehydration of the lipids and the ions but an increased hydration of the peptide, especially of its cationic moieties. Hence, in our model, various enthalpic and entropic terms, often larger in magnitude than the shift in binding free energy itself, compete by favoring or opposing the increased binding of NK-2 to PE.

Cancellation of large opposing components of the binding free energy has been observed previously for the binding of a mildly hydrophobic peptide to a hydrophobic surface [23], conformational transitions of peptide homo-dimers [25], for the binding of ligands to proteins [20–22,26–28], and for the stronger binding of NK-2 to PG compared to PC [29]. Compensation of decreased van der Waals and electrostatic interactions between the binding partners by an increased hydration of polar groups has also been revealed to play a role in the cross-reactivity of an antibody with a non-cognate ligand [26]. Our present results indicate that such effects may also contribute to the stronger binding of NK-2 to PE compared to PC.

NK-2 is an amphiphilic, highly cationic α-helical antimicrobial peptide, and thus may be considered as a typical representative for the class of α-helical antimicrobial peptides. It is thus likely that the results obtained for NK-2 here might be also relevant for a wider range of peptides. On the other hand, our results show that chemical intuition may not be sufficient for understanding antimicrobial selectivity, highlighting the need for the usage of computational methods for the design of peptide-mimetic AMPs. One promising target for extensions of the present study is to understand the dependence of the antimicrobial selectivity on the amino acid sequence, as well as on the lipid composition of prokaryotic and eukaryotic membranes, in near atomic detail.

Acknowledgements

The authors thank R. Lipowsky and S.J. Marrink for stimulating discussions and the Max Planck Society for financial support.

Appendix A. Supplementary data

Supplementary data to this article can be found online at http://dx.doi.org/10.1016/j.bbamem.2012.05.012.

References

[1] M.R. Yeaman, N.Y. Yount, Mechanisms of antimicrobial peptide action and resistance, Pharmacol. Rev. 55 (2003) 27–55.
[2] E. Fleming, N.P. Maharaj, J.L. Chen, R. Nelson, D.E. Elmore, Effect of lipid composition on buforin II structure and membrane entry, Proteins 73 (2008) 480–491.
[3] H. Leontiadou, A.E. Mark, S.J. Marrink, Antimicrobial peptides in action, J. Am. Chem. Soc. 128 (2006) 12156–12161.
[4] R. Rathinakumar, W. Walkenhorst, W.C. Wimley, Broad-spectrum antimcrobial peptides by rational combinatorial design and high-throughput screening: the importance of interfacial activity, J. Am. Chem. Soc. 131 (2009) 7609–7617.
[5] J. Pan, D.P. Tieleman, J.F. Nagle, N. Kucerka, S. Tristram-Nagle, Alamethicin in lipid bilayers: combined use of X-ray scattering and MD simulations, Biochim. Biophys. Acta 1788 (2009) 1387–1397.
[6] N.Y. Yount, A.S. Bayer, Y.Q. Xiong, M.R. Yeaman, Advances in antimicrobial peptide immunobiology, Biopolymers 84 (2006) 435–458.
[7] W. Dowhan, Molecular basis for membrane phospholipid diversity: why are there so many lipids? Annu. Rev. Biochem. 66 (1997) 199–232.
[8] P.F. Devaux, Static and dynamic lipid asymmetry in cell membranes, Biochemistry 30 (1991) 1163–1173.
[9] K. Matsuzaki, K. Sugishita, M. Harada, N. Fujii, K. Miyajima, Interactions of an antimicrobial peptide, magainin 2, with outer and inner membranes of gram-negative bacteria, Biochim. Biophys. Acta 1327 (1997) 119–130.
[10] J.D. Gehman, F. Luc, K. Hall, T.H. Lee, M.P. Boland, T.L. Pukala, J.H. Bowie, M.I. Aguilar, F. Separovic, Effect of antimicrobial peptides from australian tree frogs on anionic phospholipid membranes, Biochemistry 47 (2008) 8557–8565.
[11] F. Jean-Francois, S. Castano, B. Desbat, B. Odaert, M. Roux, M.H. Metz-Boutigue, E.J. Dufourc, Aggregation of cateslytin beta-sheets on negatively charged lipids promotes rigid membrane domains. a new mode of action for antimicrobial peptides? Biochemistry 47 (2008) 6394–6402.
[12] S. Tolokh, V. Vivcharuk, B. Tomberli, C.G. Gray, Binding free energy and counterion release for adsorption of the antimicrobial peptide lactoferricin B on POPG membrane, Phys. Rev. E 80 (2009) 31911-1–31911-12.
[13] V. Vivcharuk, B. Tomberli, I.S. Tolokh, C.G. Gray, Prediction of binding free energy for adsorption of antimicrobial peptide lactoferricin B on a POPC membrane, Phys. Rev. E 77 (2008) 31913-1–31913-11.
[14] J. Pimthon, R. Willumeit, A. Lendlein, D. Hofman, Membrane association and selectivity of the antimicrobial peptide NK-2: a molecular dynamics simulation study, J. Pept. Sci. 15 (2009) 654–667.
[15] K.A. Henzler Wildmann, D. Lee, A. Ramamoorthy, Mechanism of lipid bilayer disruption by the human antimicrobial peptide, ll-37, Biochemistry 42 (2003) 6545–6558.
[16] R. Willumeit, M. Kumpugdee, S.S. Funari, K. Lohner, B.P. Navas, K. Brandenburg, S. Linser, J. Andrä, Structural rearrangement of model membranes by the peptide antibiotic NK-2, Biochim. Biophys. Acta, Biomembr. 1669 (2005) 125–134.
[17] H. Schröder-Borm, R. Willumeit, K. Brandenburg, J. Andrä, Molecular basis for membrane selectivity of NK-2, a potent peptide antibiotic derived from NK-lysin, Biochim. Biophys. Acta, Biomembr. 1612 (2003) 164–171.
[18] M. Andersson, H. Gunne, B. Agerberth, A. Boman, T. Bergman, R. Sillard, H. Jornvall, V. Mutt, B. Olsson, H. Wigzell, A. Dagerlind, H. Boman, G. Gudmundsson, NK-lysin, a novel effector peptide of cytotoxic T-cells and NK-cells – structure and cDNA cloning of the porcine form, induction by interleucin-2, antibacterial and antitumor-activity, EMBO J. 14 (1995) 1615–1625.
[19] J. Andrä, M. Leippe, Candidacidal activity of shortened synthetic analogs of amoebapores and NK-lysin, Med. Microbiol. Immunol. 188 (1999) 117–124.
[20] L. Chong, Y. Duan, L. Wang, I. Massova, P. Kollman, Molecular dynamics and free-energy calculations applied to affinity maturation in antibody 48G7, Proc. Natl. Acad. Sci. U. S. A. 96 (1999) 14330–14335.
[21] B. Kuhn, P. Kollman, Binding of a diverse set of ligands to avidin and streptavidin: An accurate quantitative prediction of their relative affinities by a combination of molecular mechanics and continuum solvent models, J. Med. Chem. 43 (2000) 3786–3791.
[22] M. Peräkylä, N. Nordman, Energetic analysis of binding of progesterone and 5 beta-androstane-3,17-dione to anti-progesterone antibody DB3 using molecular dynamics and free energy calculations, Prot. Eng. 14 (2001) 753–758.
[23] D. Horinek, A. Serr, M. Geisler, T. Pirzer, U. Slotta, S.Q. Lud, L.A. Garrido, T. Scheibel, T. Hugel, R.R. Netz, Peptide adsorption on a hydrophobic surface results from an interplay of solvation, surface, and intrapeptide forces, Proc. Natl. Acad. Sci. U. S. A. 105 (2008) 2842–2847.
[24] V. Knecht, Model amyloid Peptide B18 monomer and dimer studied by replica exchange molecular dynamics simulations, J. Phys. Chem. B 114 (2010) 12701–12707.
[25] M. Kittner, V. Knecht, Disordered versus fibril-like amyloid beta (25–35) dimers in water: structure and thermodynamics, J. Phys. Chem. B 114 (2010) 15288–15295.
[26] P. Kar, R. Lipowsky, V. Knecht, Importance of polar solvation for cross-reactivity of antibody and its variants with steroids, J. Phys. Chem. B 115 (2011) 7661–7669.
[27] P. Kar, V. Knecht, Energetic basis for drug resistance of HIV-1 protease mutants against amprenavir, J. Comput. Aided Mol. Des. 26 (2012) 215–232.
[28] P. Kar, V. Knecht, Origin of decrease in potency of darunavir and two related antiviral inhibitors against HIV-2 compared to HIV-1 protease, J. Phys. Chem. B 116 (2012) 2605–2614.
[29] C. von Deuster, V. Knecht, Competing interactions for antimicrobial selectivity based on charge complementarity, Biochim. Biophys. Acta, Biomembr. 1808 (12) (2011) 2867–2876.
[30] I. Liepina, C. Czaplewski, P. Janmey, A. Liwo, Molecular dynamics study of a gelsolin-derived peptide binding to a lipid bilayer containing phosphatidylinositol 4,5-bisphosphate, Biopolymers 71 (2003) 49–70.
[31] K. Balali-Mood, P.J. Bond, M.S.P. Sansom, Interaction of monotopic membrane enzymes with a lipid bilayer: A coarse-grained md simulation study, Biochemistry 48 (2009) 2135–2145.
[32] C.L. Wee, K. Balali-Mood, D. Gavaghan, M. Sansom, The interaction of phospholipase a2 with a phospholipid bilayer: Coarse-grained molecular dynamics simulations, Biophys. J. 95 (2008) 1649–1657.
[33] I.S. Tolokh, V. Vivcharuk, B. Tomberli, C.G. Gray, Binding free energy and counterion release for adsorption of the antimicrobial peptide lactoferricin b on a popg membrane, Phys Rev. E 80 (031911) (2009) 031911.
[34] A. Sayyed-Ahmad, H. Khandelia, Y.N. Kaznessis, Relative free energy of binding between antimicrobial peptides and SDS or DPC micelles, Mol. Simul. 35 (2009) 986–997.
[35] J. Srinivasan, T. Cheatham, P. Cieplak, P. Kollman, D. Case, Continuum solvent studies of the stability of DNA, RNA, and phosphoramidate - DNA helices, J. Am. Chem. Soc. 120 (1998) 9401–9409.
[36] Y. Gofman, S. Linser, A. Rzeszutek, D. Shental-Bechor, S. Funari, N. Ben-Tal, R. Willumeit, Interaction of an antimicrobial peptide with membranes: Experiments and simulations with NKCS, J. Phys. Chem. B 114 (2010) 4230–4237.
[37] T. Simonson, G. Archontis, M. Karplus, Free energy simulations come of age: Protein-ligand recognition, Acc. Chem. Res. 35 (2002) 430–437.
[38] S.J. Marrink, H.J. Risselada, S. Yefimov, A.H. de Vries, The MARTINI force field: coarse grained model for biomolecular simulations, J. Phys. Chem. B 111 (2007) 7812–7824.
[39] L. Monticelli, S. Kandasamy, X. Periole, R.G. Larson, D.P. Tieleman, S.J. Marrink, The MARTINI coarse-grained force field: extension to proteins, J. Chem. Theory Comput. 4 (2008) 819–834.
[40] M.J. Hinner, S.-J. Marrink, A.H. de Vries, Location, Tilt, and Binding: A Molecular Dynamics Study of Voltage-Sensitive Dyes in Biomembranes, J. Phys. Chem. B 113 (48) (2009) 15807–15819, http://dx.doi.org/10.1021/jp907981y.
[41] G. Singh, D.P. Tieleman, Using the Wimley-White hydrophobicity scale as a direct quantitative test of force fields: the MARTINI coarse-grained model, J. Chem. Theory Comput. 7 (7) (2011) 2316–2324, http://dx.doi.org/10.1021/ct2002623.
[42] C. Olak, Biophysikalische Studien zur Wechselwirkung des antimikrobiellen Peptides NK-2 mit membranmimetischen Systemen, Ph.D. thesis, Universität Potsdam, (2008).
[43] B. Hess, H. Bekker, H.J.C. Berendsen, J.G.E.M. Fraaije, LINCS: a linear constraint solver for molecular simulations, J. Comput. Chem. 18 (1997) 1463–1472.
[44] H.J.C. Berendsen, J.P.M. Postma, W.F. van Gunsteren, A. Di Nola, J.R. Haak, Molecular-dynamics with coupling to an external bath, J. Chem. Phys. 81 (1984) 3684–3690.
[45] D. van der Spoel, E. Lindahl, B. Hess, G. Groenhof, A.E. Mark, H.J.C. Berendsen, GROMACS: Fast, flexible, and free, J. Comput. Chem. 26 (2005) 1701–1718.
[46] D. Frenkel, B. Smit, Understanding molecular simulation - from algorithms to applications, 2nd edition Academic Press, 525 B Street, Suite 1900, San Diego, California 9210–4495, USA, 2002.
[47] S. Leemkujorn, A.K. Sum, Molecular characterization of gel and liquid-crystalline structures of fully hydrated POPC and POPE bilayers, J. Phys. Chem. B 111 (2007) 6026–6033.
[48] N. Kucerka, S. Tristram-Nagle, J.F. Nagle, Structure of fully hydrated fluid phase lipid bilayers with monounsaturated chains, J. Membr. Biol. 208 (2005) 193–202.
[49] R.P. Rand, V.A. Parsegian, Hydration forces between phospholipid bilayers, Biochim. Biophys. Acta 988 (1989) 351–376.
[50] J.F. Nagle, Area lipid of bilayers from NMR, Biophys. J. 64 (1993) 1476–1481.
[51] J. MacCallum, D. Tieleman, Computer simulation of the distribution of hexane in a lipid bilayer: Spatially resolved free energy, entropy, and enthalpy profiles, J. Am. Chem. Soc. 128 (1) (2006) 125–130.
[52] C. Eun, M.L. Berkowitz, Thermodynamic and hydrogen-bonding analyses of the interaction between model lipid bilayers, J. Phys. Chem. B 114 (8) (2010) 3013–3019.
[53] D.F. Evans, H. Wennerström, The colloidal domain: where physics, chemistry, biology, and technology meet, 2nd Edition Wiley-VCH, New York, 1999.
[54] E. Lindahl, O. Edholm, Mesoscopic undulations and thickness fluctuations in lipid bilayers from molecular dynamics simulations, Biophys. J. 79 (1) (2000) 426–433.
[55] C.G. Sinn, M. Antonietti, R. Dimova, Binding of calcium to phosphatidylcholine-phosphatidylserine membranes, Colloids Surf. A Physicochem. Eng. Asp. 282 (2006) 410–419, http://dx.doi.org/10.1016/j.colsurfa.2005.10.014.
[56] V. Knecht, Z. Levine, P. Vernier, Electrophoresis of neutral oil in water, J. Colloid Interface Sci. 352 (2010) 223–231, http://dx.doi.org/10.1016/j.jcis.2010.07.002.